Crimson Publishers
Wings to the Research

Research Article

Investigation of Copper Adsorption Isotherm Models of Organo-MMT Clays

Özlem Sökmen[1]*, Nevin Çankaya[2] and Selahattin Bozkurt[2]

[1]Graduate Education Institute, Uşak University, Turkey

[2]Vocational School of Health Services, Uşak University, Turkey

ISSN: 2578-0255

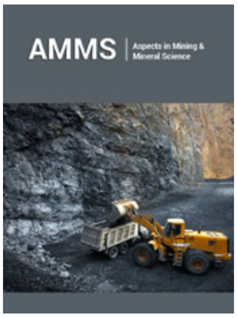

***Corresponding author:** Özlem Sökmen, Graduate Education Institute, Uşak University, 64200, Uşak, Turkey

Submission: April 14, 2026
Published: May 12, 2026

Volume 15 - Issue 1

How to cite this article: Özlem Sökmen*, Nevin Çankaya and Selahattin Bozkurt. Investigation of Copper Adsorption Isotherm Models of Organo-MMT Clays. Aspects Min Miner Sci. 15(1). AMMS. 000852. 2026.
DOI: 10.31031/AMMS.2026.15.000852

Abstract

In this study, Montmorillonite (MMT) clay, which is cheap and abundant in nature, was modified using two different modifiers. In the modification of MMT clay, 1-Butyl-3-Methylimidazolium Bromide (BMIM-Br) was used as quaternary ammonium salt and Tetraethylammonium Bromide (TEABr) was used as ionic liquid modifiers. OMMT-1, which was obtained by modifying MMT clay with BMIM-Br modifier, and OMMT-2, which was synthesized using TEABr modifier, were investigated for their use as adsorbents in the removal of Cu(II) ions from aqueous solutions. At a Cu(II) concentration of 635mg/L, OMMT-1 organoclay adsorbed 20.31% and OMMT-2 organoclay adsorbed 10.94% of Cu(II) ions. The data obtained to determine the adsorption mechanism were evaluated for their suitability according to the Langmuir, Freundlich, Temkin, Dubinin-Radushkevitch and Harkins-Jura isotherms. It was determined that the OMMT-1 organoclay obeyed the Langmuir isotherm and its maximum adsorption capacity was 38.91mg/g, while the OMMT-2 organoclay obeyed the Freundlich isotherm and its adsorption capacity, KF, was found to be 0.036. It was determined that the OMMT-1 organoclay was a better sorbent than the OMMT-2 organoclay in removing Cu(II) ions from aqueous solutions..

Keywords: Organo-montmorillonite; Cu(II) adsorption; Adsorption isotherms; Langmuir isotherm; Freundlich isotherm; RMSE

Introduction

Uncontrolled consumption, which has increased with industrialization and urbanization, is causing serious pollution of water resources. One of the pollutants commonly found in wastewater is the heavy metal copper Cu(II). Many industries, such as metal processing, electronics, chemicals, fertilizers, paper, and plastics, contain high levels of copper in their wastewater [1,2]. Copper can accumulate in living organisms without degrading and cause toxic effects. Long-term and high-level exposure to copper causes kidney dysfunction, liver disease, neurotoxicity, eye irritation, stress, depression, memory problems, muscle and joint pain, and the development of brain, skin, pancreas, and heart diseases [3,4]. Although copper is an essential element for the body, the World Health Organization has set the maximum limit for Cu(II) in drinking water at 4.0mg/L. The effective removal of biologically non-degradable copper from water is of great importance for both human health and the environment [5].

Montmorillonite (MMT) clay is a layered silicate mineral first discovered in 1696 in the Montmorillon region of France. It is usually found together with impurities such as gravel, quartz, and feldspar, and this mixture is called bentonite. MMT is obtained from bentonite using wet separation methods [6]. Structurally, it consists of layers approximately 1nm thick and 200-300nm in horizontal dimensions. The Na^+ and Ca^{2+} ions between the layers are exchanged with organic cations, making the clay organophilic. Bu Modification enhances the compatibility of MMT with hydrophobic polymers. [7,8]. MMT is an important type of clay that attracts the interest of researchers in many fields such as adsorption, catalysis, and composite material development due to its high surface area, cation exchange capacity, and excellent thermal stability. Owing to these properties, MMT has a wide range of applications in the design of sensors, filtration membranes, and membranes for lithium-ion batteries [9,10]. One of the commonly used methods for removing toxic metals from wastewater is adsorption. Although various adsorbent materials are used in this process, clay minerals stand out due to their large surface areas, high ion exchange capacities, and ability to effectively retain metal ions thanks to the negative charge in their structures. For this reason, clay minerals are among the most widely used adsorbents in wastewater treatment worldwide [11-13]. Adsorption isotherms describe the behavior and mechanism of a substance in a liquid medium adhering to a solid surface at a constant temperature and pH. These isotherms help us understand the interaction between the adsorbent and the adsorbed substance, the surface properties, and how adsorption occurs in a single layer, multiple layers, physically, or chemically. Each model has been developed to explain different adsorption conditions and characteristics [14]. Table 1 shows the isotherm models and equations used in this study [15-23].

Table 1: Adsorption isotherm models and equations.

C_o: Initial solution concentration (mg/L)

C_e: Concentration of the substance remaining in the solution after adsorption (mg/L)

q_e: Amount of substance adsorbed onto a unit adsorbent at equilibrium (mg/g)

b: A constant relating to the net enthalpy of adsorbed molecules or ions (L/mg)

q_m: The amount of adsorbed substance per unit weight of adsorbent required to form a single layer on the surface depends on the adsorption energy (mg/g)

K_F: Freundlich constant related to adsorption capacity (mg/g)

n: A constant that provides information about the shape of an isotherm.

A_T: Equilibrium binding constant corresponding to maximum binding energy (L/mg)

b_T: Temkin constant

B_T: Temkin isotherm constant related to the heat of adsorption

R: Universal gas constant (kJ/mol K)

T: Absolute temperature (K)

E: Average adsorption free energy (kJ/mol)

β : A constant related to adsorption energy

ε : D-R isotherm constant

A_H ve B_H: Harkins-Jurassic isotherm constants.

Name of the Isotherm	Linear Formula of Isotherms	Explanation
Langmuir isotherm	$\frac{C_e}{q_e}=\frac{1}{b.q_m}+\frac{C_e}{q_m}$ (1) $\frac{1}{q_e}=\frac{1}{q_m}+\left(\frac{1}{q_m b}\right)\frac{1}{C_e}$ (2)	The Langmuir isotherm model describes the adsorption of a limited number of identical regions onto a surface through single-layer adsorption. According to this model, all active sites on the surface have equal energy and affinity for adsorbed molecules [15,16]. The Langmuir isotherm constant b is a thermodynamic parameter reflecting the binding energy of ions or molecules to the adsorbent surface [8].
Freundlich isotherm	$Ln(q_e)=Ln(K_F)+\frac{1}{n}Ln(C_e)$ (3)	The Freundlich adsorption isotherm is used for heterogeneous surfaces where multi-layer adsorption occurs [17]. The value of n, one of the important parameters determining the conformity of adsorption to the Freundlich isotherm, should be in range 1<n<10 [18].
Temkin isotherm	$q_e=B(LnA)+B(LnC_e)$ (4) $B=\frac{R.T}{bT}$	The Temkin isotherm model explains that due to interactions between the adsorbent and adsorbed molecules, the heat of adsorption of the adsorbed molecules decreases linearly as the surface of the adsorbent becomes covered [19]. It is applied to estimate the average adsorption free energy (E) [20].
Dubinin-Radushkevitch isotherm (D-R)	$Lnq_e=Lnq_m-\beta\varepsilon^2$ (5) $E=\frac{1}{\sqrt{2\beta}}$	

Harkins-Jura isotherm	$\frac{1}{q_e^2} = \left(\frac{B_H}{A_H}\right) - \left(\frac{1}{A_H}\right) Log C_e$ (6)	The Harkins-Jura adsorption isotherm explains multilayer adsorption by the presence of a heterogeneous pore distribution [21,22].
RMSE	$RMSE = \sqrt{\frac{1}{N}\sum_{i=1}^{N}(calculated\ value - experimental\ value)\, i^2}$	RMSE, defined as the root mean square of the difference between model predictions and experimental data regarding adsorption capacity, is used to evaluate the accuracy of model [23].

In this study, OMMT-1 organoclay was obtained by subjecting MMT clay to a cation exchange reaction with BMIM-Br. Subsequently, OMMT-2 organoclay was synthesized by modifying MMT with TEABr. The adsorption capacities of both organoclays towards Cu(II) ions were determined, and the obtained experimental data were evaluated using various adsorption isotherm models.

Materials and Methods

In this study, Montmorillonite (MMT, <63µ) clay obtained from Esan-Eczacıbaşı was used as clay [24]. 1-Butyl-3-Methylimidazolium Bromide (BMIM-Br), Tetraethylammonium Bromide (TEABr), Ethanol (C_2H_5OH), Sodium Hydroxide (NaOH), and Hydrochloric Acid (HCl), Copper(II) Sulfate Pentahydrate ($CuSO_4 \cdot 5H_2O$), were commercially obtained from Aldrich and Fluka. All chemical reagents used in organoclay synthesis were used directly without undergoing any purification process. A UV-Vis Spectrophotometer (Shimadzu UV-1800) was used for Cu(II) determination, and no buffer or reagent was used during absorbance measurement. Weighing's were performed using an OHAUS analytical balance with a sensitivity of 0.1mg. pH measurements were performed using a Mettler Toledo (FiveEasy F20) model digital pH meter analyzer.

Synthesis of OMMT-1 and OMMT-2 organoclays

MMT clay (10g), dried in an oven at 110 °C for 48 hours, was stirred in a mixture of ethanol (30mL) and pure water (40mL) at room temperature for 1 hour. In addition, solutions of 1.97g (0.89mmol) BMIM-Br and 1.89g (0.89mmol) TEABr modifiers were prepared separately in ethanol (3mL). To obtain OMMT-1 organoclay, BMIM-Br solution was added dropwise to the MMT clay solution, and to obtain OMMT-2 organoclay, TEABr solution was added dropwise to the MMT clay solution, and the mixture was stirred at 60 °C for 24 hours [25,26]. The precipitates formed as a result of both processes were filtered, purified by washing with a hot ethanol-water mixture, and dried in an oven at 120 °C for 48 hours [25,27]. Figure 1 shows the chemical synthesis of OMMT-1 and OMMT-2 organoclays.

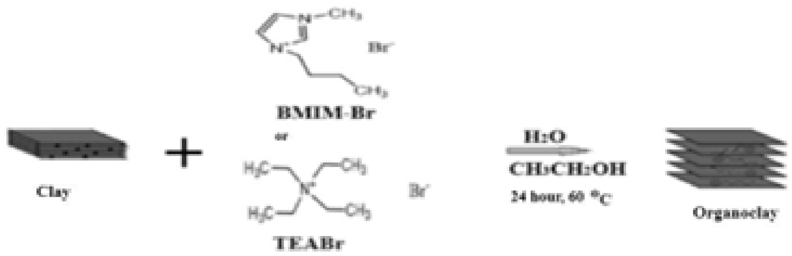

Figure 1: Chemical synthesis of OMMT-1 and OMMT-2 organoclays.

Characterization of organoclays

The spectroscopic characterization of OMMT-1 and OMMT-2 organoclays was carried out according to the literature. In the FTIR spectrum of MMT clay, O-H stretching vibrations at 3619cm^{-1}, Si-O stretching vibrations at 1003cm^{-1}, and Al-O bond vibrations at 795cm^{-1} were observed [28]. In the FTIR spectrum of OMMT-1 organoclay, ring-bound C-H stretching vibrations were observed in the 3200-3000cm^{-1} range. Additionally, aliphatic C-H stretching at 2800cm^{-1} and vibrations belonging to C≡N groups at 2191 and 2130cm^{-1} were detected. Vibrations at 1570cm^{-1} for CH_2-N and CH_3-N bonds, at 1460cm^{-1} for CH3-CN groups in the ring, at 1427cm^{-1} for C-C stretching vibrations, and at 1380cm^{-1} for C-C vibrations in the ring were observed [29,30]. The bands observed in the MMT vibration were also observed in the OMMT-2 vibration, with the aliphatic symmetric C-H vibration at 2894-2853cm^{-1}, the aliphatic asymmetric C-H vibration at 2986-2927cm^{-1}, and the CH_3 vibration at 1443cm^{-1}, as reported in the literatüre [25]. XRD analysis has determined that when MMT clay is modified with both ionic liquid and quaternary ammonium salt, the distance between clay layers increases [31,32]. Since these data are available in the literature, they have not been repeated in this study.

Discussion and Conclusion

Preparation of the calibration curve

For adsorption studies, Cu(II) solutions were prepared as fresh solutions from a stock solution containing 6355mg/L Cu(II) using $CuSO_4.5H_2O$. 1.0, 2.5, 6.0, 8.0, and 10.0mL were taken from the stock solution and diluted to 10mL with water. Thus, solutions of 635, 1588, 2541, 3812, 5083, and 6355mg/L were obtained. The obtained solutions were used to prepare a calibration graph at a wavelength of 790nm using a UV-Vis spectrophotometer (Figure 2) [24].

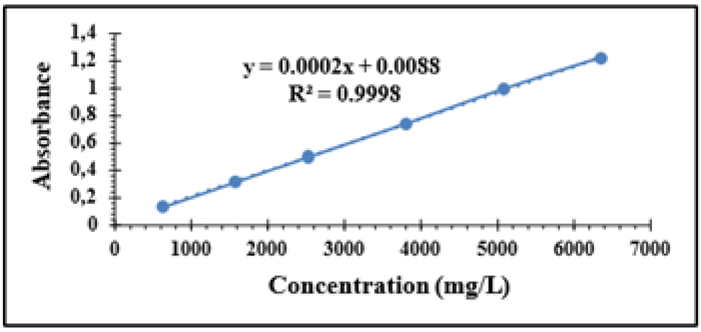

Figure 2: Calibration graph of Cu(II) solutions.

In this study, adsorption experiments were conducted at room temperature (25 °C). The effect of temperature variation on adsorption was not investigated, and parameters such as pH, adsorbent amount, and initial concentration were evaluated. Adsorption studies on the removal of Cu(II) ions using OMMT-1 and OMMT-2 organoclay materials were conducted at pH=1-3. However, it has been observed that the adsorption capacity of both organo-MMT type adsorbents for Cu(II) ions is very low. Nevertheless, the highest adsorption capacity was achieved at pH=4.5. In contact time studies conducted using a UV-Vis spectrophotometer, adsorption efficiency (%Ads) was found to be quite low. Measurements taken at different time intervals (maximum 3 hours) showed that the system did not reach equilibrium, and the optimum adsorption time was determined to be 24 hours. In this regard, measurements were taken at the end of the 24-hour contact period for each amount of adsorbent used, and evaluations were made. In determining the amount of adsorbate, pH=4.5 and room temperature were kept constant, and the value of 5083mg/L given in the calibration graph in Figure 2 was taken into account in the studies. The effects of OMMT organoclays on Cu(II) adsorption studies were evaluated using the following equations. %Ads [33,34] and the amount of Cu(II) ions retained per unit mass (q_e) [35] were calculated using the mathematical expressions given in Equations 8 and 9. Solutions containing various amounts of adsorbent material were left to stand at room temperature and pH 4.5 for 24 hours under the same experimental conditions to reach equilibrium, and the solution was decanted. Measurements were performed using the calibration graph provided in Figure 2 for the Cu(II) concentration.

$$\%Ads = \frac{(C_0 - C_e)}{C_0} \times 100 \quad (8)$$

$$q_e = \frac{(C_0 - C_e) \cdot V}{m} \quad (9)$$

A_0: Absorbance value read under UV before the solution comes into contact with the adsorbent

A_e: Absorbance value read under UV after the solution comes into contact with the adsorbent

C_0: Initial concentration of Cu(II) solutions (mg/L)

C_e: Cu(II) concentration remaining in the solution after contact with the adsorbent (mg/L)

q_e: Amount of adsorbed substance in equilibrium on the adsorbent (mg/g)

V: Volume of the solution (L)

m: The mass of adsorbent (g)

Adsorption studies

All experiments were performed in triplicate

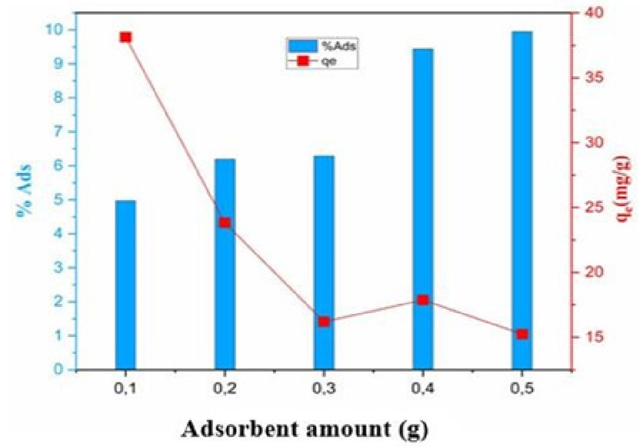

Figure 3: Effect of adsorbent amount on Cu(II) adsorption by OMMT-1 organoclay

Effect of adsorbent amount: To investigate the effect of initial amounts of organoclays on Cu(II) adsorption, 0.1, 0.2, 0.3, 0.4 and 0.5g of organoclays were weighed, respectively, and their adsorbent properties were studied using 5083mg/L Cu(II) solution (15mL) for 24 hours at 25 °C pH 4.5 (Figure 3 & 4). The data obtained are shown in Table 2.

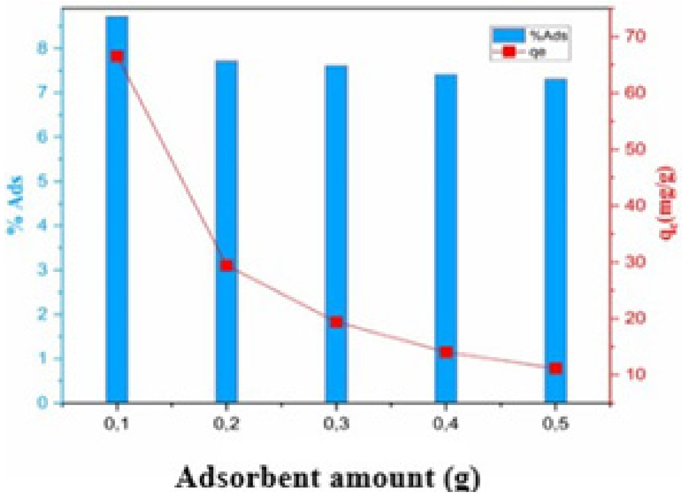

Figure 4: Effect of adsorbent amount on Cu(II) adsorption by OMMT-2 organoclay.

Table 2: Effect of adsorbent amount on Cu(II) adsorption by OMMT-1 and OMMT-2 Organoclays.

OMMT-1			OMMT-2		
Adsorbent amount (g)	**%Ads**	**qe (mg/g)**	**Adsorbent amount (g)**	**%Ads**	**qe (mg/g)**
0.1	4.98	38.12	0.1	8.73	66.72
0.2	6.19	23.83	0.2	7.28	29.55
0.3	6.29	16.20	0.3	7.65	19.38
0.4	9.44	17.87	0.4	7.53	14.30
0.5	9.95	15.25	0.5	7.40	11.25

Effect of initial concentration on Cu(II) adsorption: After determining that the best adsorption effect was achieved using 0.1g of organoclay, the effect of different Cu(II) concentrations on adsorption was investigated. For this purpose, 15mL of Cu(II) solutions at different concentrations, as given in Table 3, were each supplemented with 0.1g of OMMT-1 and OMMT-2 organoclays and the solutions were left to stand at pH 4.5 for 24 hours. The highest adsorption capacity was determined to be 5083mg/L (Table 3). The graphs for these results are presented in Figure 4 for OMMT-1 and Figure 5 for OMMT-2.

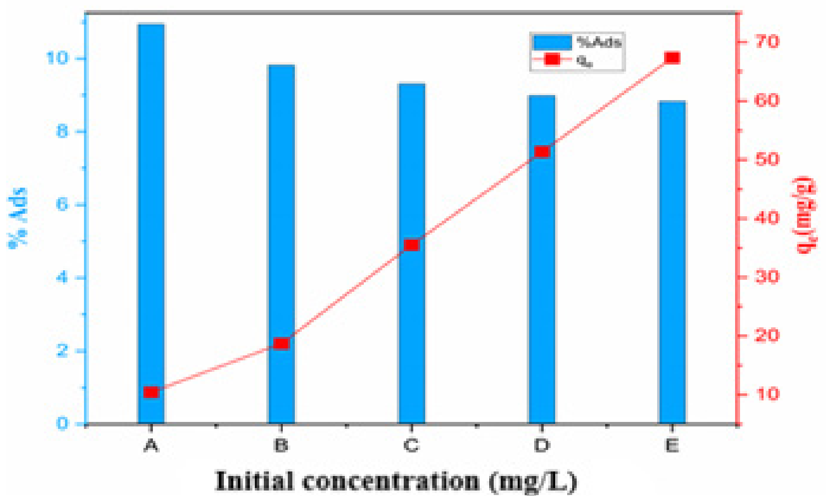

Figure 5: Effect of initial concentration on Cu(II) adsorption by OMMT-1 organoclay (A:635; B:1270; C:2541; D:3812; E:5083).

Table 3: Effect of initial concentration on Cu(II) adsorption by OMMT-1 and OMMT-2 organoclays.

OMMT-1			OMMT-2		
Initial Concentration (mg/L)	%Ads	qe (mg/g)	Initial Concentration (mg/L)	%Ads	qe (mg/g)
635	20.31	20.02	635	10.94	10.43
1270	16.73	32.41	1270	9.82	18.72
2541	6.88	26.69	2541	9.31	35.50
3812	5.71	32.41	3812	8.98	51.35
5083	4.87	37.17	5083	8.83	67.35

Adsorption isotherm results: Adsorption experiments were carried out at a constant adsorbent dosage of 0.1g, room temperature (25 °C), contact time of 24 hours, and pH=4.5. Cu(II) solutions with different initial concentrations of 635mg/L, 1270mg/L, 2541mg/L, 3812mg/L, and 5083mg/L were prepared (Figure 6). The Cu(II) adsorption behavior of OMMT-1 and OMMT-2 organoclays was evaluated using the Langmuir, Freundlich, Temkin, D-R, and Harkins-Jura isotherm models, and the corresponding plots are presented in Figure 7. The constants obtained from these adsorption isotherms are given in Table 4. The RMSE values calculated to evaluate the fit of different isotherm models are given in Table 5.

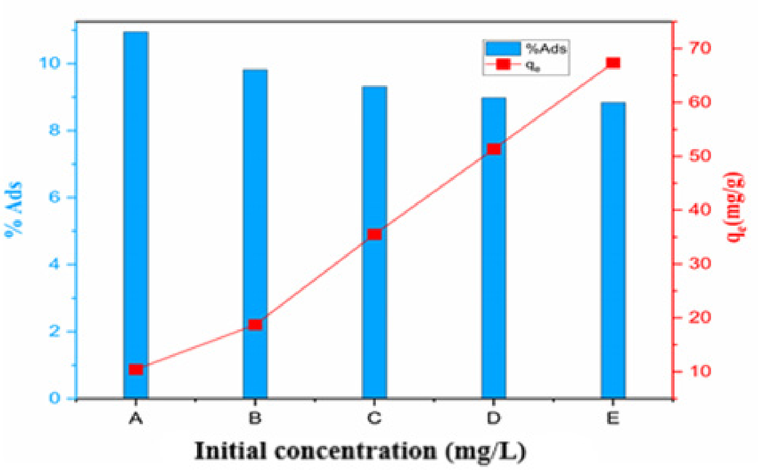

Figure 6: Effect of initial concentration on Cu(II) adsorption by OMMT-2 organoclay (A:635; B:1270; C:2541; D:3812; E:5083).

Table 4: Cu(II) adsorption isotherm graphs of OMMT-1 and OMMT-2 organoclays.

Adsorption Isotherms	Isotherm Constants	OMMT-1 Organoclay	OMMT-2 Organoclay
Langmuir	q_m (mg/g)	38.91	166.67
	b (L/mg)	0.00184	0.00012
	R^2	0.9595	0.9970
Freundlich	K_F (mg/g)	6.12	0.036
	n	4.83	1.12
	R^2	0.6408	0.9995
Temkin	A_T	0.107	0.00214
	B_T	5.622	26.355
	b_T	4.346	0.927
	R^2	0.6277	0.9328
D-R	q_m (mg/g)	33.09	46.02
	E	0.0491	0.0241
	β	206.35	864.32
	R^2	0.7381	0.7920
Harkins-Jura	A_H	714.28	106.38
	B_H	4.29	3.56
	R^2	0.6505	0.8491

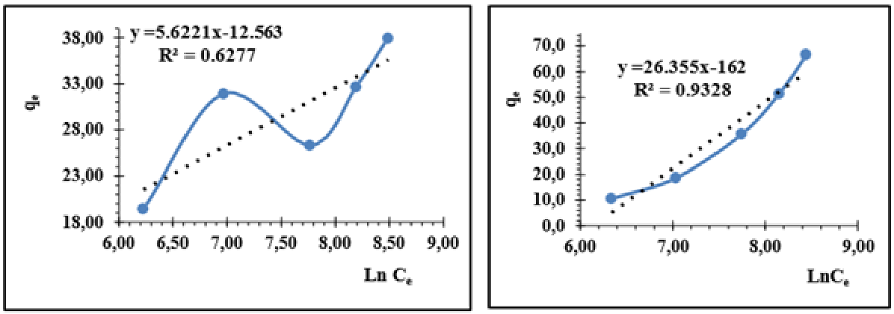

Temkin isotherm Temkin isotherm

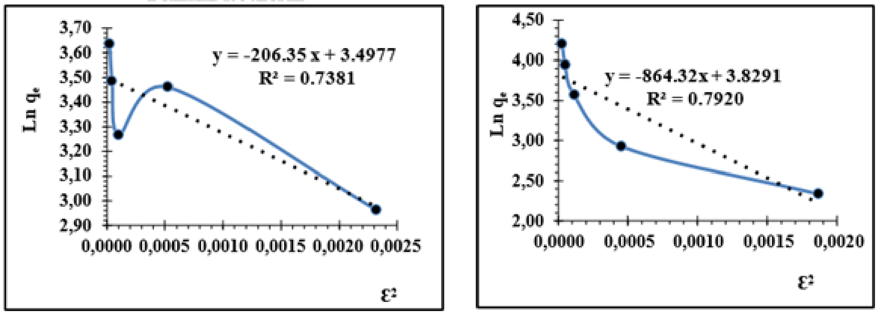

D-R isotherm D-R isotherm

Figure 7: Cu(II) adsorption isotherm graphs of OMMT-1 and OMMT-2 organoclays.

Table 5: RMSE values of OMMT-1 and OMMT-2 organoclays in different isotherm models.

Isotherm Model	RMSE for OMMT-1 (mg/g)	RMSE for OMMT-2 (mg/g)
Langmuir	3.92	3.72
Freundlich	3.61	0.85
Temkin	3.59	5.41
D-R	30.31	11.24
Harkins-jura	4.20	42.16

In adsorption studies, pH affects adsorption efficiency by altering the surface properties of the adsorbent. Ma et al. [36] stated that the low amount of Cu(II) ions adsorbed by the adsorbent at low pH could be explained by the adsorption competition between H+ and Cu(II) ions. They reported that when the pH of the solution is increased, the competition between H+ and Cu(II) ions decreases, leading to an increase in the number of negatively charged regions on the adsorbent, which in turn increases the Cu(II) adsorption efficiency. In this study, pH=4.5 was preferred for adsorption studies because it was observed that Cu(II) ions precipitated as $Cu(OH)_2$ when pH>5. In the literature [5], [37] it has been reported that copper metal precipitates as $Cu(OH)_2$ at pH values above 6.

When OMMT-1 and OMMT-2 were used, the highest adsorption capacity (q_e) for Cu(II) adsorption was observed when 0.1g of organoclay was used (Table 2). These values were found to be 38.12mg/g for 0.1g of OMMT-1 and 66.72mg/g for OMMT-2. Additionally, it was observed that q_e values decreased with increasing adsorbent amount in both types of organoclay. In accordance with the literature [38-40] it was determined that there was no significant change in %Ads values at the end of 24 hours when the system reached equilibrium. In this study, adsorption experiments conducted with both OMMT-1 and OMMT-2 organoclays revealed a decrease in q_e values, which represent the amount of metal ions absorbed per unit mass, as the amount of adsorbent increased. This situation has been previously reported in the literature by Ekinci & İlter [41] and is consistent with the explanation that an increase in adsorbent quantity may lead to the active regions on the adsorbent surface not being fully saturated, thereby causing a decrease in adsorption capacity [41]. Similarly, Mellouk et al. [38] stated in their study using different amounts of organoclay that the use of high amounts of adsorbent did not significantly change the adsorption capacity of Cu(II) ions and preferred 2.5g as the optimal adsorbent amount in their subsequent experiments. These literature findings are consistent with our experimental data and indicate that increasing the adsorbent amount may limit adsorption efficiency under certain conditions.

The effect of the initial concentration of Cu(II) ions on the adsorption capacity and %Ads was investigated. The highest adsorption capacity was observed at an initial concentration of 5083mg/L (Table 3), and the adsorption capacity corresponding to this value was determined to be 37.17mg/g for OMMT-1 and 67.35mg/g for OMMT-2. Although a significant increase in adsorption capacity was observed with increasing initial concentration, a decrease in %Ads values was observed due to the limited number of active sites on the surface. As the initial Cu(II) ion concentration increases, the amount adsorbed (q_e) increases due to the presence of more metal ions in the solution. The observed decrease in the adsorption percentage (%Ads) is due to the limitation of active adsorption areas on the adsorbent surface over time and the approach to surface saturation [41].

Cu(II) adsorption of OMMT-1 and OMMT-2 organoclays was evaluated according to Langmuir, Freundlich, Temkin, D-R and Harkins-Jura isotherms. Table 4 shows the Cu(II) adsorption isotherm constants of OMMT-1 and OMMT-2 organoclays. The Langmuir isotherm was found to be the most suitable isotherm for the OMMT-1 organoclay due to its R^2 value of 0.9595, the small difference between the experimental q_e and the calculated q_m, and the RMSE value of 3.92, which is a small value when comparing the adsorption isotherm models given in Table 5. In the case of OMMT-2 organoclay, the most suitable model was found to be the Freundlich model, as evidenced by the R^2 value of 0.9995, the n value representing the adsorption capacity of 0.036, and the RMSE value of 0.85 given in Table 5, [42]. When the isotherm constants given in Table 4 & 5 are ranked from most suitable to least suitable, the Langmuir>Freundlich>Temkin>Harkins-Jura>D-R isotherm was determined for OMMT-1. The most suitable isotherm model ranking for OMMT-2 has been determined as Freundlich>Langmuir>Temkin>D-R>Harkins-Jura. The fact that different isotherm models fit experimental data to varying degrees stems from each model being based on different fundamental assumptions regarding the adsorption process. The findings from this study show that the adsorption of Cu(II) ions onto the organoclay surface is based on electrostatic interactions resulting from increased surface negativity under pH=4.5 conditions [43-45].

It is considered that weak physical interactions such as Van der Waals forces contribute to the adsorption process at a secondary level in interlayer regions. The adsorption mechanism is based on pH-dependent electrostatic attractions and weak Van der Waals interactions originating from the modified clay surface. However, due to the pH dependence of electrostatic interactions, this mechanism is only effective within certain pH ranges and cannot be considered the primary determinant of adsorption under all pH conditions. This situation reveals that adsorption efficiency varies depending on surface charge and environmental pH values. In studies on Cu(II) adsorption in MMT clays modified with different modifiers in the literature, it has been observed that the adsorption isotherms most closely follow the Langmuir and Freundlich isotherms (Table 6).

Table 6: Adsorption of Cu(II) by different types of clay adsorbents.

Adsorbent	Maximum Adsorption Capacity	Optimal Adsorption Isotherm	Sources
Gemini (containing four ammonium cations)/MMT organoclay	34.33mg/g	Langmuir	[43]
Ca-Bentonite	55.48mg/g	Langmuir	[44]
SDS/MMT/Fe-hydrate organoclay	20.56mg/g	Langmuir	[13]
Saudi MMT clay	32.36mg/g	Langmuir	[45]
Fe-MMT	48.08mg/g	Langmuir	[46]
Organobentonite	0.22mmol/g	Langmuir	[47]
Hexadecyltrimethylammonium bromide-MMT	7.53mg/g	Langmuir	[48]
Bentonite clay	52.63mg/g	Langmuir Freundlich	[49]
OMMT-1	39.91mg/g	Langmuir	This study
OMMT-2	0.036	Freundlich	

Result

In this study, two different types of organoclays, OMMT-1 and OMMT-2, were synthesized using commercially available MMT clay. The adsorption of Cu(II) ions was investigated using these synthesized organoclays in different amounts, and the adsorption effect against different Cu(II) ion concentrations was examined with the amount of the best adsorbent material determined. In adsorption studies, the fit of synthesized organoclays to the Langmuir, D-R, Freundlich, Temkin, and Harkins-Jura adsorption isotherm models was investigated [46-49]. The OMMT-1 organoclay follows the Langmuir isotherm due to its high R2 and low RMSE value compared to other models. Accordingly, it was determined that OMMT-1 conforms to the Langmuir model, possessing equal energy regions and a homogeneous adsorbent surface, and that Cu ions adhere to the adsorbent surface in a single layer. Furthermore, since the n value is in the range 1<n<10 and the R2 value is 0.9970, which is high compared to other models, it has been observed that the surface of OMMT-2 has a heterogeneous and multi-layered structure in accordance with Freundlich. Due to the hydrophobic nature of the synthesized OMMT-1 and OMMT-2 organoclays and their increased adsorption capacity when used in composite form, it is predicted that they can be used for the effective removal of organic and metallic pollutants in wastewater.

Acknowledgement

We would like to thank the Uşak University Scientific Research Projects Unit (Project No: 2017/TP018)

for their support of this thesis study. This study is derived from Özlem Sökmen’s doctoral thesis at Uşak

University, Graduate School of Education, Department of Chemistry.

References

1. Adeeyo RO, Bello OS (2014) Use of composite sorbents for the removal of copper (II) ions from aqueous solution. Pakistan Journal of Analytical and Environmental Chemistry 15(2): 1-12.
2. Ahmad R, Kumar R, Haseeb S (2012) Adsorption of Cu^{2+} from aqueous solution onto iron oxide coated eggshell powder: Evaluation of equilibrium, isotherms, kinetics, and regeneration capacity. Arabian Journal of Chemistry 5(3): 353-359.
3. Hasana NH, Wahi R, Yusof Y, Yusof WRW, Manan ZAA (2020) Coconut shell biochar for removal of Cu(II) from aqueous solution. Pakistan Journal of Analytical & Environmental Chemistry 21(2): 280-292.
4. Böck FC, Helfer GA, Costa AB, Dessuy MB, Ferrao MF (2022) Low-cost method for copper determination in sugarcane spirits using photometrix UVC® embedded in smartphone. Food Chemistry 367: 130669.
5. Maity J, Ray SK (2017) Removal of Cu(II) ion from water using sugar cane bagasse cellulose and gelatin based composite hydrogels. International Journal of Biology Macromolecules 97: 238-248.
6. Pillai SK, Ray SS (2012) Chitosan-based nanocomposites. Natural Polymers. Royal Society of Chemistry, Cambridge UK.
7. Cole G, Gok MK, Guçlu G (2013) Removal of basic dye from aqueous solutions using a novel nanocomposite hydrogel: n-vinyl 2-pyrrolidone/itaconic acid/organo clay. Water Air Soil Pollution 224(11): 1760.
8. Ouellet-Plamondon C, Lynch RJ, Al-Tabbaa A (2012) Comparison between granular pillared, organo- and inorgano-organo-bentonites for hydrocarbon and metal ion adsorption. Applied Clay Science 67-68: 91-98.
9. Alekseeva O, Noskov A, Grishina E, Ramenskaya L, Kudryakova N, et al. (2019) Structural and thermal properties of montmorillonite/ionic liquid composites. Materials 12(16): 2578.
10. Lertsutthiwong P, Noomun K, Khunthon S, Limpanart S (2012) Influence of chitosan characteristics on the properties of biopolymeric chitosan-montmorillonite. Progress in Natural Science: Materials International 22(5): 502-508.
11. Peighambardoust SJ, Bavil OA, Foroutan R, Arsalani N (2020) Removal of malachite green using carboxymethyl cellulose-g-polyacrylamide/montmorillonite nanocomposite hydrogel. International Journal of Biological Macromolecules 159: 1122-1131.
12. Otunola BO, Ololade OO (2020) A review on the application of clay minerals as heavy metal adsorbents for remediation purposes. Environmental Technology and Innovation 18: 100692.
13. Li SZ, Wu PX (2010) Characterization of sodium dodecyl sulfate modified iron pillared montmorillonite and its application for the removal of aqueous Cu(II) and Co(II). Journal of Hazardous Materials 173(1-3): 62-70.
14. Aladağ E (2023) Optimization of nonlinear adsorption ısotherm models by error analysis. Journal of the Institute of Science and Technology 13(1): 200-212.
15. Si R, Chen Y, Wang D, Yu D, Ding Q, et al. (2022) Nanoarchitectonics for high adsorption capacity carboxymethyl cellulose nanofibrils-based adsorbents for efficient Cu^{2+} removal. Nanomaterials 12: 160.
16. Sharma G, Kumar A, Ghfar AA, García-Peñas A, Naushad M, et al. (2022) Fabrication and characterization of xanthan gum-cl-poly(acrylamide-co-alginic acid) hydrogel for adsorption of cadmium ions from aqueous medium. Gels 8: 23.
17. Tirtom VN, Dinçer A (2021) Effective removal of heavy metals from an aqueous solution with poly (N- vinylimidazole-acrylamide) hydrogels. Separatıon Science and Technology 56(5): 912-924.
18. Altınay G, Levent M (2023) Removal of Ni(II) from industrial wastewater via adsorption and characterization of selected adsorbents. Usak University Journal of Science and Natural Sciences 7(1): 1-13.
19. Erdoğdular AO, Apar DK (2021) Biosorption of reactive dye remazol ultra red RGB by metabolically active kefir biomass. Journal of the Faculty of Engineering and Architecture of Gazi University 36(2): 1055-1073.
20. Periyasamy S, Manivasakan P, Jeyaprabha C, Meenakshi S, Viswanathan N (2019) Fabrication of nano-graphene oxide assisted hydrotalcite/chitosan biocomposite: An efficient adsorbent for chromium removal from water. International Journal of Biological Macromolecules 132: 1068-1078.
21. Kar F, Yılgın M, Duranay N (2019) Determination of adsorption parameters in removal of methylene blue from aqueous solution using activated zeolite and polyvinylpyrrolidone. Duzce University Journal of Science and Technology 7: 1-14.
22. Onursal N, Dal MC (2023) Investigation of isotherm and thermodynamic parameters of adsorption of copper (II) ions in aqueous solution with natural mixed type Siirt clay (NMTSC-2) and new (second) linear equation derived from Harkins-Jura isotherm. Chemical Papers 78: 749-760.
23. Gümüş D, Gümüş F (2024) Removal of crystal violet dye from aqueous solution by a modified adsorbent; Optimum isotherm with linear and nonlinear model equations, kinetic and design. The Black Sea Journal of Sciences 14(4): 2227-2243.
24. Sökmen O, Çankaya N (2023) Remediation of toxic Cu(II) with acrylamide-based hydrogels. Advances in Clinical Toxicology 8(3): 000278.
25. Borisover M , Bukhanovsky N, Lapides I , Yariv S (2010) Mild pre-heating of organic cation- exchanged clays enhances their interactions with nitrobenzene in aqueous environment. Adsorption 16: 223-232.
26. Li Z, Jiang WT, Chang PH, Lv G, Xu S (2014) Modification of a Ca-montmorillonite with ionic liquids and its application for chromate removal. Journal of Hazardous Materials 270: 169-175.
27. Arora A, Choudhary V, Sharma D (2011) Effect of clay content and clay/surfactant on the mechanical, thermal and barrier properties of polystyrene/organoclay nanocomposites. Journal of Polymer Research 18(4): 843-857.
28. Cankaya N, Sahin R (2019) Chitosan/clay bionanocomposites: Structural, antibacterial, thermal and swelling properties. Cellulose Chemistry and Technology 53(5 6): 537-549.
29. Burba CM, Singh DK, Chiou YW, Wang TH, Chang HC (2023) Pressure-dependent cationic associations of ionic liquids with bentonite nanoclay. Journal of Ionic Liquids 3(2): 100067.
30. Grishina EP, Ramenskaya LM, Kudryakova NO, Vagin KV, Kraev AS, et al. (2019) Composite nanomaterials based on 1-butyl-3-methylimidazolium dicianamide and clays. Journal of Materials Research and Technology 8(5): 4387-4398.
31. Tagac AA, Bozaci E (2024) Application of ionic liquid-clay nanocomposites on cotton fabric and determination of multi-functional properties. Cellulose 31(16): 9979-10006.
32. Yalçınkaya SE, Yıldız N, Saçak M, Çalımlı A (2010) Preparation of polystyrene/montmorillonite nanocomposites: Optimization by response surface methodology (RSM). Turkish Journal of Chemistry 34: 581-592.
33. Zango ZU, Garba ZN, Abu Bakar NHH, Tan WL, Abu Bakar M (2016) Adsorption studies of Cu^{2+}–Hal nanocomposites for the removal of 2,4,6-trichlorophenol. Applied Clay Science 132-133: 68-78.
34. Duan L, Hu N, Wang T, Wang H, Ling L, et al. (2016) Removal of copper and lead from aqueous solution by adsorption onto cross-linked chitosan/montmorillonite nanocomposites in the presence of hydroxyl-aluminum oligomeric cations: equilibrium, kinetic, and thermodynamic studies. Chemical Engineering Communications 203: 28-36.
35. Kasgoz H, Ozbas Z, Esen E, Sahin CP, Gurdag G (2013) Removal of copper(II) ions with a thermoresponsive cellulose-g-poly(n-isopropyl

acrylamide) copolymer. Journal of Applied Polymer Science 130(6): 4440-4448.

36. Ma L, Zhu J, Xi Y, Zhu R, He H, et al. (2016) Adsorption of phenol, phosphate and Cd(II) by inorganic organic montmorillonites: A comparative study of single and multiple solute. Colloids and Surfaces A: Physicochemical and Engineering Aspects 497: 63-71.
37. Zhao B, Jiang H, Lin Z, Xu S, Xie J, et al. (2019) Preparation of acrylamide/acrylic acid cellulose hydrogels for the adsorption of heavy metal ions. Carbohydrate Polymers 224: 115022.
38. Mellouk S, Belhakem A, Khelifa KM , Schott J, Khelifa A (2011) Cu(II) adsorption by halloysites intercalated with sodium acetate. Journal of Colloid and Interface Science 360: 716-724.
39. Arlayıcı SP, Altun T (2018) Removal of chromium (VI) from aqueous solutions using chitosan coated kaolıne beads as adsorbent. Selcuk Univ J Eng Sci Tech 6(1): 140-151.
40. Onursal N (2023) Removal of Ni (II) from aqueous solutions by bionanocomposite produced from waste almond shell. MAS Journal of Applied Sciences 8(2): 391-402.
41. Ekinci S, İlter Z (2021) Investigation of the adsorption of Cr (III) ions by MNPs-G1-Mu adsorbent prepared with iron oxide nanoparticles modified with polyamidoamine dendrimer. Nevşehir Bilim ve Teknoloji Dergisi 10(2): 111-123.
42. Dautoo UK, Shandil Y, Ranote S, Jamwal S, Chauhan GS (2022) New efficient poly(acrylic acid)-based bifunctional Cu^{2+} ions adsorbents. Colloids and Surfaces A: Physicochemical and Engineering Aspects 635: 128090.
43. Ouakouak A, Rihani K, Youcef L, Hamdi N, Guergazi S (2020) Adsorption characteristics of Cu (II) onto $CaCl_2$ pretreated algerian bentonite. Materials Research Express 7: 025045.
44. Chu Y, Khan MA, Zhu S, Xia M, Lei W (2019) Microstructural modification of organo-montmorillonite with Gemini surfactant containing four ammonium cations: molecular dynamics (MD) simulations and adsorption capacity for copper ions. Journal of Chemical Technology and Biotechnology 94(11): 3585-3594.
45. Alandis NM, Mekhamer W, Aldaye O, Hefne JAA, Alam M (2019) Adsorptive applications of montmorillonite clay for the removal of Ag(I) and Cu(II) from aqueous medium. Journal of Chemistry 1-4: 1-7.
46. Cruz JK, Diaz LJ (2019) Adsorption of Cu(II) onto Fe(III)-modified montmorillonite-kinetic, isotherm, and thermodynamic studies. IOP Conference Series: Materials Science and Engineering 540: 1-9.
47. Neto AFA, Vieira MGA, Silva MGC (2012) Cu(II) Adsorption on modified bentonitic clays: different isotherm behaviors in static and dynamic systems. Materials Research 15(1): 114-124.
48. Bendezú Y, Fuentes WS (2019) Use of nanoclay as an adsorbent to remove Cu(II) from acid mine drainage (AMD). Chemical Engineering Transactions 73: 241-246.
49. Şenol H, Açıkel U (2018) Investigation of adsorption of Cu (II) heavy metal with bentonite. Bitlis Eren University Journal of Science and Technology 7(2): 231-242.